THE UNIVERSITY of EDINBURGH

Edinburgh Research Explorer

The Hydroxamate Siderophore Rhequichelin Is Required for Virulence of the Pathogenic Actinomycete Rhodococcus equi

OPEN ACCESS

The Hydroxamate Siderophore Rhequichelin Is Required for Virulence of the Pathogenic Actinomycete *Rhodococcus equi*

Raúl Miranda-CasoLuengo,[a] Garry B. Coulson,[b] Aleksandra Miranda-CasoLuengo,[a] José A. Vázquez-Boland,[c,d] Mary K. Hondalus,[b] and Wim G. Meijer[a]

UCD School of Biomolecular and Biomedical Science and UCD Conway Institute, University College Dublin, Dublin, Ireland[a]; Department of Infectious Diseases, University of Georgia, Athens, Georgia, USA[b]; Microbial Pathogenesis Unit, Edinburgh Infectious Diseases and Centre for Immunity, Infection and Evolution, University of Edinburgh, Edinburgh, United Kingdom[c]; and Grupo de Patogenómica Bacteriana, Facultad de Veterinaria e Instituto de Biología Molecular y Genómica, Universidad de León, León, Spain[d]

We previously showed that the facultative intracellular pathogen *Rhodococcus equi* produces a nondiffusible and catecholate-containing siderophore (rhequibactin) involved in iron acquisition during saprophytic growth. Here, we provide evidence that the *rhbABCDE* cluster directs the biosynthesis of a hydroxamate siderophore, rhequichelin, that plays a key role in virulence. The *rhbC* gene encodes a nonribosomal peptide synthetase that is predicted to produce a tetrapeptide consisting of N^5-formyl-N^5-hydroxyornithine, serine, N^5-hydroxyornithine, and N^5-acyl-N^5-hydroxyornithine. The other *rhb* genes encode putative tailoring enzymes mediating modification of ornithine residues incorporated into the hydroxamate product of RhbC. Transcription of *rhbC* was upregulated during growth in iron-depleted medium, suggesting that it plays a role in iron acquisition. This was confirmed by deletion of *rhbCD*, rendering the resulting strain *R. equi* SID2 unable to grow in the presence of the iron chelator 2,2-dipyridyl. Supernatant of the wild-type strain rescued the phenotype of *R. equi* SID2. The importance of rhequichelin in virulence was highlighted by the rapid increase in transcription levels of *rhbC* following infection and the inability of *R. equi* SID2 to grow within macrophages. Unlike the wild-type strain, *R. equi* SID2 was unable to replicate *in vivo* and was rapidly cleared from the lungs of infected mice. Rhequichelin is thus a key virulence-associated factor, although nonpathogenic *Rhodococcus* species also appear to produce rhequichelin or a structurally closely related compound. Rhequichelin biosynthesis may therefore be considered an example of cooption of a core actinobacterial trait in the evolution of *R. equi* virulence.

The genus *Rhodococcus*, which contains over 40 species, is widely distributed in the environment, including in soil (3). The enormous metabolic diversity of these species is exploited in a large number of biotechnological applications, ranging from bioremediation of soils to production of fine chemicals (3, 45). *Rhodococcus equi*, the only animal pathogen in this genus, proliferates rapidly as a saprophyte in soil, especially when these soils are enriched with manure of grazing herbivores (2, 20). *R. equi* is a multihost pathogen infecting a wide range of animals as well as humans. However, as the name implies, *R. equi* is predominantly an equine pathogen, in particular of young foals, which become infected in the first 6 months of life (31, 48). Equine *R. equi* disease most frequently presents as pyogranulomatous cavitating pneumonia, while ulcerative enteritis and osteomyelitis are also common manifestations (31, 48). The success of *R. equi* as a pathogen depends on its ability to prevent phagosomal maturation and the production of microbicidal compounds following uptake by phagocytic cells (19, 43). *R. equi* subsequently proliferates within these compartments, eventually killing the macrophage in a necrotic manner (16, 26). Proliferation in macrophages and development of disease in foals are dependent on VapA, a member of the virulence-associated protein (Vap) family encoded within a pathogenicity island of the virulence plasmid (18, 21).

Iron plays a critical role as an electron carrier and biocatalyst and is therefore an essential micronutrient in most bacteria. While iron is abundant in nature, it is usually present as Fe^{3+}, which is insoluble at neutral pH in aerobic environments (1). In animals iron is sequestered by proteins such as lactoferrin and transferrin or is bound to heme. In addition, mammals respond to infection by further lowering the iron concentration as part of the acute-phase response (35). The concentration of free iron both in soil and in the host is therefore too low to sustain bacterial growth.

To gain access to iron, many saprophytic and pathogenic bacteria produce siderophores, a structurally diverse group of low-molecular-weight compounds that are characterized by an extremely high affinity for iron (51). The majority of siderophores have hydroxamate, catecholate, or carboxylate iron coordinating groups; however, mixed siderophores that have more than one type of functional group have also been identified (12, 51). Siderophores may be produced by nonribosomal peptide synthetases (NRPS) or by NRPS-independent pathways (9, 12). Following chelation of Fe^{3+} in the medium, siderophores are taken up by their cognate ABC transport systems, and Fe^{3+} release subsequently occurs either by reduction of Fe^{3+} to Fe^{2+} or by hydrolysis of the siderophore (23, 25, 28).

We previously demonstrated that *R. equi* produces a diffusible catecholate-containing siderophore (rhequibactin) during growth in iron-depleted medium (30). The synthesis of

TABLE 1 Bacterial strains and plasmids used in this study

Strain or plasmid	Genotype or characteristics	Source or reference
Strains		
E. coli DH5α	*supE44* D*lacU169* (φ*lacZ*ΔM15) *hsdR17 recA1 endA1 gyrA96 thi-1 relA1*	Bethesda Research Laboratories
R. equi		
ATCC 33701	Virulent strain, 81-kb virulence plasmid p33701	American Type Culture Collection
ATCC 33701 P-	Avirulent strain, virulence plasmid cured	41
SID2sc	Single-crossover derivative of ATCC 33701 containing pSid2K inserted into *rhbCD*	This study
SID2	Double-crossover derivative of SID2sc resolving into deletion of *rhbCD*	This study
SID2rev	Double-crossover derivative of SID2sc resulting in the regeneration of *rhbCD*	This study
Plasmids		
pSelAct	Ap^r *lacZ codA::upp*	44
pSid2K	pSelAct derivative containing the upstream region of *rhbC* (coordinates 788716–790175) and the downstream region of *rhbD* (coordinates 808254–809630) producing an in-frame deletion of *rhbCD*	This study

rhequibactin depends on a six-cistron operon containing two NRPS genes, *iupS* and *iupT*, and four genes encoding siderophore biosynthesis and transport proteins. Upstream and transcribed divergently of this operon is a four-cistron operon encoding enzymes required for the production of 2,3-dihydroxybenzoic acid, which is also present in the mixed-type catecholate-hydroxamate siderophores heterobactin A, rhodobactin, and rhodochelin produced by *R. erythropolis*, *R. rhodochrous*, and *R. jostii*, respectively (4, 7, 14). In addition to rhequibactin, *R. equi* appears to synthesize a nonsoluble siderophore that is produced by an NRPS protein encoded by *iupU* (30). While disruption of either *iupS* or *iupU* prevented growth of *R. equi* in medium supplemented with the iron chelator 2,2-dipyridyl, it did not attenuate *R. equi* (30).

This work analyzed the *rhbABCDE* gene cluster, which, based on a bioinformatic analysis, is predicted to direct the synthesis of a tetrapeptide hydroxamate siderophore, rhequichelin. We show here that this putative siderophore is essential for virulence of *R. equi* as judged by its requirement for bacterial proliferation in macrophages and mice.

MATERIALS AND METHODS

Bacterial strains, plasmids, and growth conditions. Bacterial strains and plasmids used in this study are listed in Table 1. Bacteria were grown at 37°C in brain heart infusion both (BHI), in Luria-Bertani (LB) broth (40), or in polypropylene flasks in minimal medium (22) supplemented with 20 mM L-lactate. Water used for minimal medium was treated with Chelex-100 ion-exchange resin to remove iron as directed by the manufacturer (Bio-Rad). Vishniac-Santer trace elements (46) with FeSO$_4$ were added for iron-replete medium (LMM), whereas they were left out for iron-depleted medium (LMM−Fe). The iron content in media was determined by atomic absorption spectroscopy in a SpectrAA-10 instrument (Varian Inc.) using an Fe^{3+} SpectroSol solution as the standard. The iron concentration in iron-replete medium (LMM) was determined to be 3.71 ± 0.28 μM (*n* = 4), whereas the iron concentration of LMM−Fe was below the assay's detection limit (0.6 μM). WT-Spent medium was produced by passing the supernatant of the wild-type strain grown in LMM−Fe to early stationary phase through a 0.22-μm filter. Where appropriate, the following supplements were added: apramycin, 30 μg · ml$^{−1}$ (*Escherichia coli*) or 80 μg · ml$^{−1}$ (*R. equi*), 5-bromo-4-chloro-3-indolyl-β-D-galactopyranoside (X-Gal), 20 μg · ml$^{−1}$; and isopropyl-β-D-thiogalactoside (IPTG), 0.1 mM. Agar (1.5%, wt/vol) was added for solid media.

DNA manipulations. Chromosomal DNA was isolated as previously described (32). Plasmid DNA was isolated using the Wizard Plus SV miniprep system (Promega) as described by the manufacturer. DNA-modify-

ing enzymes were used according to the manufacturer's recommendations (New England BioLabs). GoTaq (Promega) and Phusion (New England BioLabs) DNA polymerases were used as directed by the manufacturers for analytical and preparative PCR amplification of DNA, respectively. Other DNA manipulations were carried out using standard procedures (40).

Mutant construction. Two DNA fragments flanking the site of the intended deletion were amplified by PCR using oligonucleotide pair Sid2_1481AF and Sid2_1481AR and oligonucleotide pair Sid2_1397BF and Sid2_1397BR (Table 2). Primers Sid2_1481AR and Sid2_1397BF were designed to contain an EcoRI site. Following digestion with EcoRI and subsequent ligation, the resulting ligation product was amplified using primers Sid2_1481AF and Sid2_1397BR, which contained XbaI and ApaI restriction sites, respectively. The resulting amplicon was digested with these restriction enzymes and subsequently cloned into the corresponding restriction sites in pSelAct to generate plasmid pSID2K.

R. equi was electroporated with pSID2K as described previously (27), and single crossovers were selected in 80 μg · ml$^{−1}$ apramycin-containing LB plates. Double crossovers were obtained by counterselection with 5-fluorocytosine as previously reported (44), and the loss of the plasmid was confirmed by apramycin sensitivity. Excision of the plasmid by homologous recombination produced either the deletion mutant, *R. equi* SID2, or the revertant wild-type strain, *R. equi* SID2rev. The genotypes of the mutant and revertant strains were confirmed by PCR analysis using primer pairs that are complementary to sequences within (SID2_210F and SID2_210R) and outside (SID2_205EF and 210_205ER) the deleted region. The presence of the virulence plasmid in wild-type, mutant, and revertant strains was confirmed by amplification of *vapA* using primer pair VapA_182F and VapA_182R (Table 2).

RNA isolation. RNA was isolated from *R. equi* grown *in vitro* as described previously (39). *R. equi* RNA was isolated from macrophages following phagocytosis of the pathogen using a guanidine thiocyanate-based lysis buffer (4 M guanidine thiocyanate, 0.5% [wt/vol] sodium *N*-lauryl sarcosine, 25 mM sodium citrate, and 0.1 M β-mercaptoethanol) as previously described (6, 37). Samples were vortexed and passed 10 times through a 21-gauge needle to shear macrophage DNA and to reduce viscosity. Intracellular bacteria were recovered by 30 min of centrifugation (3,220 × *g*). Pelleted bacteria were lysed using TRIzol (Sigma) and physically disrupted with zirconia beads in a MagNALyser instrument (Roche). Total RNA was isolated by chloroform extraction followed by DNA digestion with Turbo DNase (Ambion) and application to a Qiagen RNeasy column, with a second, in-column, DNA digestion with the RNase-free DNase as previously described (29).

Reverse transcription and reverse transcription-PCR (RT-PCR). cDNA was produced by extension of hexameric random primers with Improm-II reverse transcriptase and 1U/μl RNasin RNase inhibitor using

TABLE 2 Oligonucleotides used in this study

| Oligonucleotide	Nucleotide sequence	Purpose	Source or reference
7610F	TCGTGATCCGAGTCGAGAA	*rhbABCDE* transcriptional organization	This study
7620R	CGTCACCCTTGACCTGGTAG	*rhbABCDE* transcriptional organization	This study
7620F	CTACCAGGAGATTCCCGACA	*rhbABCDE* transcriptional organization	This study
7630R	GACGAGGATCTCGGACTGC	*rhbABCDE* transcriptional organization	This study
7630F	ACACGCGTACTTCGAGTTCT	*rhbABCDE* transcriptional organization	This study
7640R	ATCAGGTCGAGCGTCTCCT	*rhbABCDE* transcriptional organization	This study
7640F	CGAGAAGACTCACGGACTGA	*rhbABCDE* transcriptional organization	This study
7650R	GAGTGCTGGTCCTCATCGTT	*rhbABCDE* transcriptional organization	This study
SID2_1481AF	CGATCTCTAGACGAGTCGTGGATGTTGAGG	Construction of pSid2K	This study
SID2_1481AR	CTAGGAATTCGGTTGTAGACGGTGCTCTGC	Construction of pSid2K	This study
SID2_1397BF	CTCGGAATTCGATGAGCACCAATCCGTTC	Construction of pSid2K	This study
SID2_1397BR	ATATGGGCCCTATCGGTCGATGGACTTCA	Construction of pSid2K	This study
SID2_210F	CACTTCGTGTCCCAGTTCCT	Genotyping of the SID2 mutant and qPCR of *rhbC*	This study
SID2_210R	GTAGGTCAACCGCAGGTCTC	Genotyping of the SID2 mutant and qPCR of *rhbC*	This study
SID2_205EF	GTATGTCTGCGGATCACCTG	Genotyping of the SID2 mutant	This study
SID2_205ER	AGTGCTGGTCCTCATCGTTG	Genotyping of the SID2 mutant	This study
VapA_182F	AATGCGACCGTTCTTGATTC	Amplification of *vapA*	30
VapA_182R	TCTCCGTGAACGTCGTACTG	Amplification of *vapA*	30
SID3_205F	TTGGGTATTCACCACCTCGT	qPCR of *iupS*	30
SID3_205R	CGAGGTAGTCGGTCCAGAAC	qPCR of *iupS*	30
SID1_220F	CCTCCCTATCTCGTGGAACA	qPCR of *iupU*	30
SID1_220R	CCTCCCCGTACACGTACAAC	qPCR of *iupU*	30
SID4_193F	GGGGCTGCCACTACCTCAGTA	qPCR of *iupT*	30
SID4_193R	CTTACGCGGACGGAAACAC	qPCR of *iupT*	30
16SrRNA200F	ACGAAGCGAGAGTGACGGTA	qPCR of the 16S rRNA gene	29
16SrRNA200R	ACTCAAGTCTGCCCGTATCG	qPCR of the 16S rRNA gene	29

80 ng of total RNA following the manufacturer's directions (Promega). DNA contamination of RNA samples was ruled out by including controls with no addition of reverse transcriptase. Endpoint PCR was performed using oligonucleotides listed in Table 2 and KAPA2G Fast DNA polymerase following the manufacturer's instructions (Kapa Biosystems).

qPCR and analysis of data. Quantitative PCR (qPCR) using appropriate oligonucleotides (Table 2) was performed using the hot-start Light-Cycler 480 SYBR green I Master as recommended by the manufacturer. Samples were subjected to 45 cycles of 94°C for 15 s, 60°C for 15 s, and 72°C for 15 s with temperature transition rates of 4.2, 2.2, and 4.2°C/s, respectively. A melting curve analysis from 50 to 99°C (temperature transition, 0.2°C/s) was performed after amplification. At least two independent experiments in duplicate were performed for each sample. The efficiency of amplification (E) was determined for each pair of primers with the equation $E = 10^{(1/-s)}$, where s is the slope of the standard curve. Fold changes were calculated using the $E^{\Delta\Delta CT}$ method. 16S rRNA was used as a reference for normalization. Absolute quantification of transcripts made use of standard curves of known amounts of template DNA in the range of 10^2 to 10^7 molecules.

Eukaryotic cell cultures. Macrophage-like J774A.1 cells (ATCC TIB-67) were grown in Dulbecco modified Eagle medium (DMEM) supplemented with 10% (vol/vol) fetal bovine serum and 2 mM L-glutamine and grown at 37°C with 5% CO_2. Primary bone marrow-derived macrophages were obtained from femurs and tibias of BALB/c mice (Charles River, Wilmington, MA) aged 6 to 8 weeks by flushing with 5 ml each of cold phosphate-buffered saline (PBS) (without $CaCl_2$ and $MgCl_2$) supplemented with penicillin-streptomycin (10 units · ml^{-1} penicillin and 10 mg · ml^{-1} streptomycin) and collected in 50-ml conical tubes. The cells were spun for 10 min at 1,100 rpm. The supernatant was discarded, and the cell pellet was resuspended in 24 ml per mouse of DMEM, 10% (vol/vol) fetal calf serum (FCS), 10% (vol/vol) CSF-1 conditioned supernatant, and 2 mM glutamine. The cells were plated in 6-well non-tissue-culture-treated plates (4 ml/well) and incubated at 37°C with 5% CO_2. On day 3, a further 4 ml/well medium was added, and cells were incubated for an-

other 3 days. On day 6, nonadherent cells were removed by aspiration of the medium, and adherent cells were washed once with 4 ml PBS. Adherent cells were then resuspended by addition of 8 ml/well cold PBS and incubation of plates at 4°C for 15 min. After incubation, any remaining adherent cells were gently resuspended using a sterile cell scraper. Cells were subsequently transferred to sterile 50-ml tubes and spun at 1,100 rpm for 10 min. The resulting pellet was suspended in medium composed of DMEM, 10% (vol/vol) FCS, 10% (vol/vol) CSF-1 conditioned supernatant, and 2 mM glutamine. The total cell number was determined by using a hemocytometer, and the cell concentration was adjusted to obtain 2×10^6 cells · ml^{-1}. These cells were then used directly for macrophage assays or frozen in 90% (vol/vol) FCS containing 10% (vol/vol) dimethyl sulfoxide (DMSO) in liquid nitrogen till further use.

Macrophage infections. Both macrophage-like J774A.1 cells and primary bone marrow macrophages were used to perform infection assays to compare the intracellular proliferation of *R. equi* and its derivative mutant *R. equi* SID2. Macrophages were seeded at 2×10^5 cells per well into 24-well tissue culture plates. Overnight broth cultures of bacteria at an optical density at 600 nm of 1.0 (2×10^8 CFU ml^{-1}) were pelleted, washed once with PBS, and resuspended in PBS. Macrophage monolayers were washed once with warm DMEM, and the medium was replaced with fresh DMEM supplemented with 10% (vol/vol) FCS, 10% (vol/vol) CSF-1 conditioned supernatant, and 2 mM glutamine. Bacteria were added at a multiplicity of infection (MOI) of 10 bacteria per macrophage. Bacterial incubation with macrophages proceeded for 60 min at 37°C, followed by repeated washing of the macrophage monolayer with prewarmed DMEM to remove unbound bacteria. The medium was subsequently replaced with complete DMEM supplemented with amikacin sulfate (20 μg · ml^{-1}), and the infected cells were incubated at 37°C in the presence of 5% CO_2. At various times postinfection, macrophage monolayers were washed repeatedly, and 500 μl sterile water was then added to lyse the macrophages upon further incubation at 37°C for 20 min. Bacterial growth was determined by dilution plating of macrophage lysates. CFU were enumerated after 1 h, 24 h, 48 h, and 72 h postinfection.
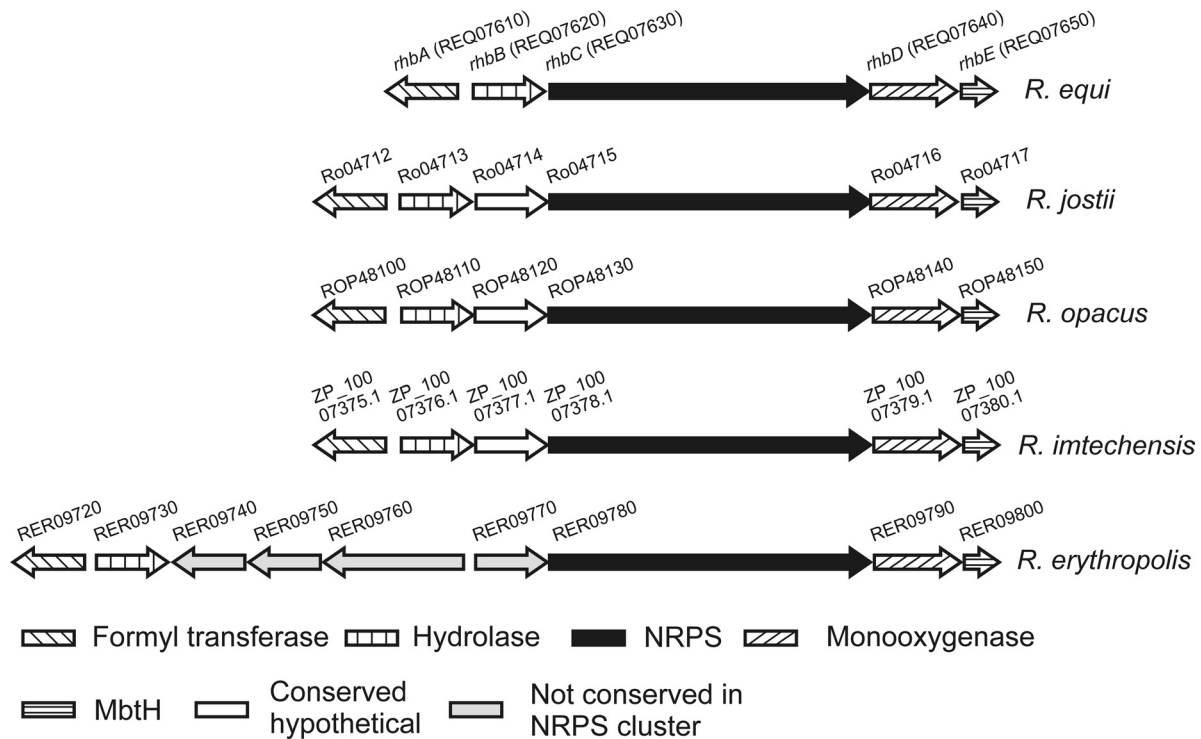
FIG 1 Schematic representation of the *rhbABCDE* cluster of *R. equi* and syntenic regions in other rhodococcal species. Genes are not drawn to scale. The sequences are derived from *R. equi* (NC_014659), *R. jostii* (NC_008268), *R. opacus* (NC_012522), *R. erythropolis* (NC_012490), and *R. imtechensis* (NZ_AJJH01000171 contig 168_1).

For the intramacrophage gene expression analysis, J774A.1 cells were seeded at 6×10^5 cells ml^{-1} in a 6-cm tissue culture plate (Sarstedt) and cultured overnight at 37°C with 5% CO$_2$. Bacteria grown in BHI broth were harvested by centrifugation (10 min, $3,220 \times g$) in the exponential phase of growth and were washed twice with cation-free PBS. J774A.1 cells were infected with *R. equi* at an MOI of 20 bacteria per macrophage. Infections were initiated by centrifugation ($160 \times g$, 3 min) of bacteria onto confluent macrophage monolayers to synchronize internalization. The first samples were harvested 1 h after addition of medium supplemented with vancomycin (5 μg · ml^{-1}), which was considered $t = 0$ h. Infected monolayers were also harvested at different time points until 48 h postinfection. Fold changes in transcript level were normalized to that of the 16S rRNA gene in qPCRs as described above.

Infection of mice. Female severe combined immunodeficient (SCID) mice were obtained from Charles River (Wilmington, MA). Mice were received at 6 weeks of age and were used when they were approximately 8 weeks old. For the infection of mice, frozen aliquots of the bacterial strains for which titers had been determined were thawed and grown for 1 h at 37°C in BHI broth. Bacteria were pelleted and resuspended in PBS at the desired concentration. Groups of mice were infected intravenously through the tail vein with approximately 5×10^5 bacteria. The concentration of the injection stock was determined retrospectively by dilution plating. To confirm that the mice received the expected amounts of bacteria, the first group of mice was sacrificed 2 h after infection. This time was defined as $t = 0$ h. At that time and at 2 and 14 days postinfection, five mice from each group were euthanized, and their livers, spleens, and lungs were removed. Each organ was placed in sterile PBS and homogenized with a tissue homogenizer (Seward, Bohemia, NY). Serial 10-fold dilutions of the homogenate were plated onto BHI agar, and CFU counts were determined after 48 h of incubation at 37°C.

Statistical analysis. Statistical analyses were performed using the SigmaPlot statistical package (SigmaPlot version 11.2.0.5; Systat Software, San Jose, CA). Comparison of the means of intracellular bacterial num-

bers between bacterial strains was assessed using a one-way analysis of variance (ANOVA). When appropriate, multiple pairwise comparisons were done using Tukey's honestly significant difference (HSD) test. Significance was set at a P value of <0.05.

RESULTS

Identification of a hydroxamate siderophore biosynthetic gene cluster. We previously showed that *R. equi* produces a diffusible catecholate-containing siderophore (rhequibactin) while growing under iron-limiting conditions, requiring the activity of IupS (REQ08140) (30). Disruption of the *iupS* gene abolished growth in the presence of the iron chelator 2,2-dipyridyl yet did not affect intracellular growth of the *iupS* mutant in macrophages. This suggested that *R. equi* deploys an additional siderophore that allows the pathogen to obtain iron during infection (30).

In order to identify additional genes that may direct the synthesis of a siderophore, a bioinformatic analysis of the *R. equi* genome was carried out, which identified a gene cluster ranging from REQ07620 to REQ07650 (24) (Fig. 1). Considering the small intergenic space between these genes, it is highly likely that this gene cluster is transcribed as a four-cistron operon. mRNA isolated from *R. equi* grown under iron-depleted conditions was reverse transcribed, and the resulting cDNA was amplified by PCR using oligonucleotide primers complementary to sequences in adjacent genes (Fig. 2). This demonstrated that the genes REQ07620 to REQ07650 form an operon. An amplicon was not observed when oligonucleotides that were complementary to REQ07610 and REQ07620, which are divergently transcribed, were used (Fig. 2).

REQ07630 encodes a 596-kDa protein that is homologous to
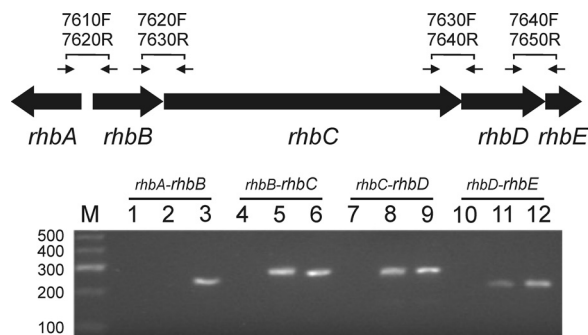
FIG 2 Transcriptional organization of the *rhbABCDE* cluster. Shown are the results of the reverse transcriptase analysis of the *rhbABCDE* cluster using oligonucleotide pairs (Table 2) 7610F/7620R (predicted size, 241 bp) complementary to *rhbA* and *rhbB* (lanes 1 to 3), 7620F/7630R (predicted size, 280 bp) complementary to *rhbB* and *rhbC* (lanes 4 to 6), 7630F/7640R (predicted size, 282 bp) complementary to *rhbC* and *rhbD* (lanes 7 to 9), and 7640F/7650R (predicted size, 221 bp) complementary to *rhbD* and *rhbE* (lanes 10 to 12). Lanes 1, 4, 7, and 10, control reactions without reverse transcriptase; lanes 2, 5, 8, and 11, 1 μl of the reverse transcriptase reaction mixture (cDNA); lanes 3, 6, 9, and 12, reactions using genomic DNA as a template. Lane M, molecular size standard in base pairs. Genes are not drawn to scale.

the exochelin-producing NRPS enzymes FxbB and FxbC of *Mycobacterium smegmatis* (52, 53). It contains four adenylation (A) domains that are required for incorporation of amino acids into the peptide assembly line. The amino acids lining the active site of the A domain of an NPRS module define the amino acid specificity of the NRPS protein (11). Challis et al. identified eight amino acids in the active site that may be used to predict which amino acid is activated by the A domain (10). The eight-amino-acid fingerprint of the A domain of the first (D_{648}, I_{649}, N_{652}, Y_{691}, W_{717}, G_{719}, G_{742}, I_{750}) and third (D_{3690}, M_{3691}, E_{3694}, N_{3732}, L_{3760}, G_{3762}, L_{3785}, I_{3793}) NPRS modules of REQ07630 are identical to A domains that bind, respectively, N^5-formyl-N^5-hydroxyornithine in module 1 of FxbB and N^5-hydroxyornithine in A domains 1 and 3 of FxbC, as identified by Challis et al. (10). The amino acids that are activated by A domains 2 and 4 were predicted to be serine and N^5-acyl-N^5-hydroxyornithine by NRPSpredictor2 (38). The REQ07630 protein therefore appears to synthesize a hydroxamate that is predicted to consist of N^5-formyl-N^5-hydroxyornithine, serine, N^5-hydroxyornithine, and N^5-acyl-N^5-hydroxyornithine.

The genes flanking REQ07630 encode putative enzymes that are likely required for modification and activation of the amino acids that are incorporated in the hydroxamate compound produced by REQ07630 and the release of this compound from the NRPS (Fig. 1). REQ07640 encodes a putative L-ornithine-5-monooxygenase that most likely is responsible for hydroxylation of L-ornithine to N^5-hydroxyornithine. REQ07650 encodes an MbtH-like protein, a protein family that was recently shown to form an integral part of NRPS synthetases and play a role in amino acid activation (15). REQ07620 encodes an α/β-hydrolase fold protein that may play a role as a thioesterase to release hydroxamate from the NRPS synthetase at the end of the assembly line. The gene upstream and transcribed divergently of the putative hydroxamate biosynthetic operon (REQ07610) is annotated as encoding a methionyl-tRNA formyltransferase, which may play a role in the synthesis of N^5-formyl-N^5-hydroxyornithine, the likely substrate of NRPS module 1.

The predicted activities of the proteins encoded by the gene cluster
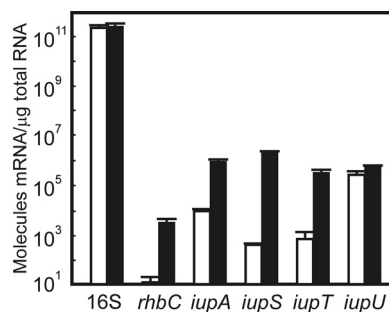
FIG 3 Transcriptional regulation of genes encoding siderophore-producing NRPS (*rhbC*, *iupS*, *iupT*, and *iupU*) (30) and a siderophore ABC transporter (*iupA*) (29) in response to the iron concentration in the medium. *R. equi* was grown in iron-replete LMM medium (white bars) or in iron-depleted LMM−Fe medium (black bars). Shown are the averages from two independent experiments in which each sample was analyzed in duplicate. Error bars denote the standard error of the mean.

encompassing REQ07610 to REQ07650 are consistent with the biosynthesis of a hydroxamate siderophore (rhequichelin). We therefore propose to use the nomenclature *rhb* (<u>rh</u>equichelin <u>b</u>iosynthesis) for REQ07610 (*rhbA*), REQ07620 (*rhbB*), REQ07630 (*rhbC*), REQ07640 (*rhbD*), and REQ07650 (*rhbE*).

Transcription of *rhbC* is regulated by iron. Transcription of the rhequibactin biosynthetic genes *iupS* and *iupT*, as well as that of the *iupABC* operon, which encodes a siderophore uptake system, is upregulated when *R. equi* is grown in medium containing low iron concentrations (29, 30), highlighting their role in iron acquisition. *R. equi* was grown in LMM (iron replete) and LMM−Fe (iron depleted) to determine whether *rhbC* transcription is also controlled by the concentration of iron. Transcription of the *rhbC* gene was clearly regulated by the iron concentration in the medium, since *rhbC* transcript levels increased more than 1,000-fold during growth in iron-depleted medium compared to iron-replete medium (Fig. 3). As was observed previously, the transcription levels of *iupS*, *iupT*, and *iupA* increased by two to three orders of magnitude following growth of *R. equi* in LMM−Fe compared to growth in LMM, whereas transcription levels of *iupU* and 16S rRNA were not affected (29, 30) (Fig. 3).

***rhbCD* is required for growth at low iron concentrations.** In silico analysis of the *rhb* gene cluster strongly suggested that it is required for the production of a hydroxamate siderophore, which is supported by the observation that transcription of *rhbC* is dependent on the concentration of iron in the medium. To further analyze the function of the *rhb* gene cluster, *rhbCD* was deleted from the genome. Initially plasmid pSid2K was inserted into the genome via a single recombination event, rendering the resulting *R. equi* strain resistant to apramycin. The correct integration of pSid2K into *rhbCD* in an apramycin-resistant first recombinant colony was confirmed by PCR (data not shown). A subsequent second recombination between the integrated plasmid and chromosome leads to excision of the plasmid. In the resulting apramycin-sensitive strains, either *rhbCD* is deleted or the wild-type genotype is restored. Phenotypic analysis showed that all of the double recombinants in which *rhbCD* was deleted were unable to grow in the presence of an 80 μM concentration of the iron chelator 2,2-dipyridyl (data not shown). In contrast, growth of all of the recombinants that reverted to the wild-type genotype was indistinguishable from that of the parent wild-type strain. Thus,
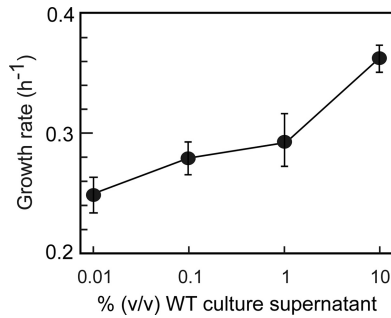
FIG 4 *R. equi* produces a diffusible compound that stimulates growth of *R. equi* SID2 under iron-limiting growth conditions. *R. equi* SID2 was grown in iron-depleted LMM−Fe medium to which filtered culture supernatant of the *R. equi* wild-type (WT) strain grown in LMM−Fe was added. The growth rates shown are the averages from three independent experiments. Error bars denote the standard error of the mean.
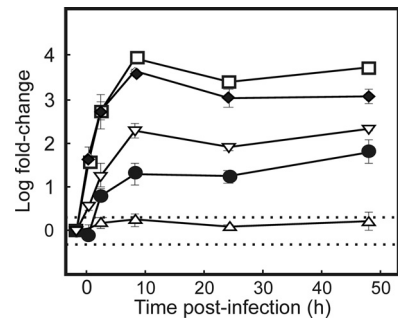

FIG 5 Transcriptional profile of genes encoding siderophore-producing NRPS proteins following infection of the murine macrophage-like cell line J774A.1. Monolayers were infected with *R. equi*; following a 1 h incubation to allow phagocytosis, monolayers were washed and treated with vancomycin to kill remaining extracellular bacteria (*t* = 0 h). ●, *iupA*; ▽, *rhbC*; △, *iupU*; □, *iupT*; ◆, *iupS*. Transcript fold changes were normalized against the levels of expression of 16S rRNA and calibrated to time 0 h. Dashed lines indicate 2-fold changes in gene expression. The experiment was carried out in triplicate. Error bars denote the standard error of the mean.

the phenotype of the Δ*rhbCD* deletion mutants is unlikely to be due to secondary mutations that could have occurred elsewhere on the genome during the gene disruption process. Growth of the *rhbCD* deletion strain *R. equi* SID2 in the presence of 2,2-dipyridyl was restored when $FeSO_4$ was added to the medium, demonstrating that lack of growth was due not to 2,2-dipyridyl toxicity but to iron limitation. The data are therefore entirely consistent with the notion that *rhbCD* is required for the production of a siderophore that supports *R. equi* growth under iron-limiting growth conditions.

rhbCD is required for the production of a diffusible siderophore. The data suggested that the *rhbABCDE* cluster directs the synthesis of a diffusible hydroxamate siderophore. To test this hypothesis, filtered culture supernatant of the *R. equi* wild-type strain grown in LMM−Fe (WT-Spent medium) was added to iron-depleted culture medium (LMM−Fe) of *R. equi* SID2. The addition of WT-Spent medium increased the maximum growth rate (μ_{max}) of *R. equi* SID2 in a dose-dependent manner, increasing from $0.26 \pm 0.1\ h^{-1}$ to $0.36 \pm 0.1\ h^{-1}$, which is comparable to that of the wild-type strain in iron-depleted medium ($\mu_{max} = 0.39 \pm 0.1\ h^{-1}$) (Fig. 4). Addition of culture supernatant of the wild type to that of *R. equi* SID2 is thus able to rescue the iron-deficient phenotype of the latter. This demonstrates that *R. equi* secretes a diffusible compound that is required for growth under iron-limiting growth conditions, which supports the hypothesis that *rhbCD* is required for the production of a siderophore.

Transcription of rhbC is upregulated in macrophages. Uptake of *R. equi* by phagocytic cells reduces access of the pathogen to essential nutrients, including iron. In order to acquire sufficient iron for growth, it is highly likely that *R. equi* adapts to this environment by upregulating the transcription of genes required for iron acquisition, including *rhbC*. To determine whether this is the case, the macrophage-like cell line J774.A1 was infected with *R. equi*, and at various time points postinfection the transcription levels of the iron acquisition genes *iupA*, *iupS*, *iupT*, *iupU*, and *rhbC* were analyzed by RT-qPCR. The transcription levels of *rhbC* increased 100-fold within 10 h postinfection, indicating that *R. equi* experiences iron limitation following uptake by macrophages. Except for *iupU*, the transcription levels of the other iron acquisition genes also increased in this period (Fig. 5).

The rhbCD genes are required for intracellular growth of R. equi. Upregulation of *rhbC* transcription in macrophages may

suggest that the *rhbABCDE* cluster is required for intracellular growth and virulence of *R. equi*. In order to test this hypothesis, bone marrow-derived macrophages were infected with wild-type *R. equi*, *R. equi* SID2, and *R. equi* SID2rev. The intracellular levels of the wild-type strain and the revertant strain *R. equi* SID2rev increased 9-fold at 72 h postinfection. In contrast, *R. equi* SID2 was significantly ($P = 0.015$) attenuated in its ability to proliferate in macrophages (Fig. 6). Similar results were obtained when the macrophage-like cell line J774 was infected with wild-type *R. equi*, *R. equi* SID2, and *R. equi* SID2rev (data not shown). These data thus show that *rhbCD* is essential for intracellular proliferation of *R. equi*.

rhbCD is required for bacterial proliferation *in vivo*. Having demonstrated that the *rhbCD* gene cluster was required for opti-
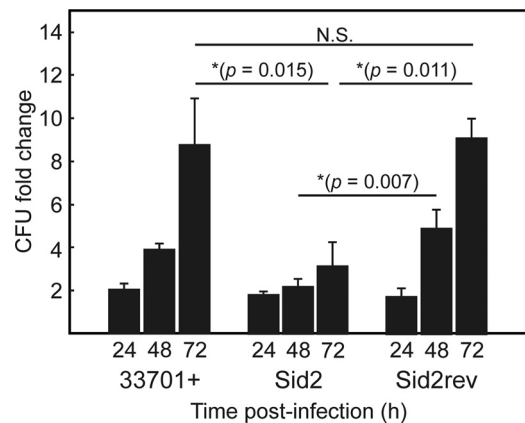
FIG 6 *R. equi* SID2 is attenuated in intracellular growth in macrophages. Bone marrow-derived macrophage monolayers were infected with wild-type *R. equi*, *R. equi* SID2, and *R. equi* SID2rev; following a 1-h incubation to allow phagocytosis, monolayers were washed and treated with amikacin to kill remaining extracellular bacteria. Intracellular bacteria were enumerated via dilution plating of macrophage lysates, and results are expressed as fold change in bacterial numbers relative to *t* = 0 (h) values. *, $P \leq 0.05$. The error bars reflect the standard deviation from the mean (SD) of values obtained from triplicate monolayers. The data shown are representative of two independent experiments.
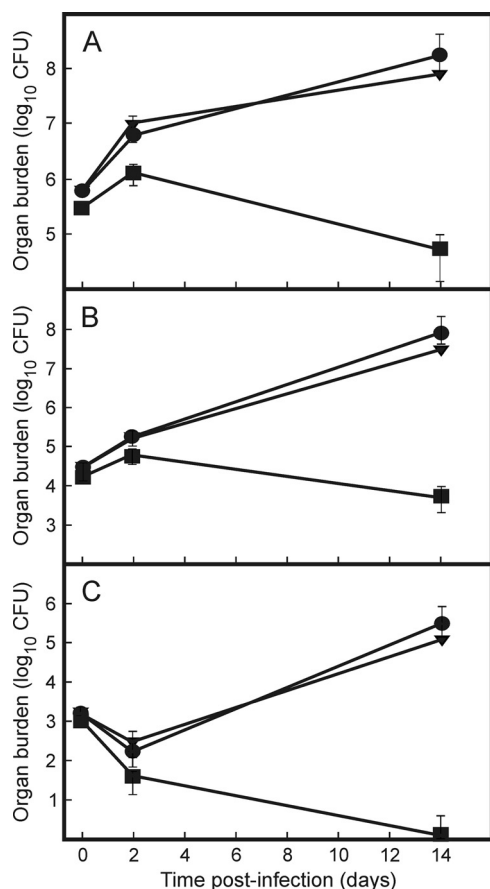
FIG 7 Clearance profile of *R. equi* SID2 in SCID mice. Eight-week-old female SCID mice were infected intravenously through the tail vein with approximately 5×10^5 CFU of *R. equi* ATCC 33701 (●), *R. equi* SID2rev (▼), and *R. equi* SID2 (■). Organs were removed aseptically at 0, 2, and 14 days to determine the total number of bacteria in liver (A), spleen (B), and lungs (C). Each point represents the mean ± SD (error bars) of bacterial counts from five mice.

mal proliferation of *R. equi* in macrophages, we speculated that it may be essential for replication *in vivo* as well. To investigate whether this was indeed the case, SCID mice were infected with the *R. equi* SID2 mutant and its *in vivo* clearance profile was followed and compared to that of wild-type *R. equi* and the SID2rev strain. At various times postinfection, five mice from each group were humanely sacrificed and microbial burdens in liver, spleen, and lungs were determined. The numbers of both the *R. equi* wild-type and SID2rev strains increased by two to three orders of magnitude in liver, spleen, and lungs at 14 days postinfection. In sharp contrast, *R. equi* SID2 numbers were reduced by one to two orders of magnitude in liver and spleen and were cleared from the lungs in the same period (Fig. 7). These data thus demonstrate that *rhbCD* is required not only for growth in macrophages but also for proliferation *in vivo*.

DISCUSSION

We previously showed that *R. equi* produces a soluble catecholate-containing siderophore, rhequibactin, and a nondiffusible siderophore (29, 30). Disruption of *iupS* and *iupU*, required for biosynthesis of the former and latter compounds, respectively, prevented growth under iron-limiting conditions but did not attenuate vir-

ulence in macrophages or mice, strongly suggesting that *R. equi* produces a third siderophore that provides the pathogen with iron following infection (29, 30). Our analysis of the *R. equi* genome identified a gene cluster, *rhbABCDE*, that may direct the biosynthesis of this siderophore. The *rhbBCDE* genes form a four-cistron operon, whereas *rhbA* is located upstream and transcribed divergently from this operon (Fig. 2). The transcription of *rhbC* was controlled by the concentration of iron in the medium, increasing 1,000-fold in iron-depleted compared to iron-replete medium. A similar observation was made for the *iupS* and *iupT* genes, encoding NRPS proteins required for the biosynthesis of the catecholate containing siderophore rhequibactin (30).

RhbC is an NRPS protein that is predicted to synthesize a tetrapeptide composed of a serine and three modified ornithine residues (N^5-formyl-N^5-hydroxyornithine, serine, N^5-hydroxyornithine, and N^5-acyl-N^5-hydroxyornithine). The rhodococcal siderophores characterized to date (heterobactin A, rhodobactin, and rhodochelin) all contain ornithine or modified ornithine residues (4, 7, 14). The remaining genes in this gene cluster are predicted to encode proteins required for the modification of ornithine by formylation and hydroxylation (RhbA and RhbD), amino acid activation (RhbE), and release of the tetrapeptide from the NRPS (RhbB).

A survey of rhodococcal genomes shows that *R. jostii*, *R. erythropolis*, *R. imtechensis*, and *R. opacus* contain a region syntenic to the *rhbABCDE* gene cluster (Fig. 1). The NRPS proteins encoded by these syntenic regions share a high degree of identity with RhbC (62 to 67%) and have the same domain structure. An analysis of the four adenylation domains of these proteins (see Table S1 in the supplemental material) showed that the active-site residues conferring substrate specificity are identical in A domains 1, 3, and 4. These domains activate modified ornithine residues for incorporation in the resulting hydroxamate. The active-site residues in A domain 2 of the *R. jostii*, *R. opacus*, and *R. imtechensis* NRPS proteins are identical to each other. They differ in active-site residue 5 compared to RER0980 of *R. erythropolis* and in residues 3 and 5 in RhbC (see Table S1 in the supplemental material). Despite these differences, NRPSpredictor2 (36, 38) predicts that A domain 2 in all five proteins activates a serine for incorporation in the resulting hydroxamate. Interestingly, the genetic organization of the NRPS loci of *R. jostii*, *R. opacus*, and *R imtechensis*, which have identical active-site residues in all four A domains, is also identical (Fig. 1). The organization of the NRPS loci of *R. equi* and *R. erythropolis*, which differ slightly in their A domain 2 active sites from the former three species, is also different from these three (Fig. 1). The conserved genetic context of the NRPS-encoding genes, in which the same tailoring enzymes are encoded, and the identical active-site residues in A domains 1, 3, and 4 and highly similar residues in A domain 2 of the NRPS proteins suggest that it is likely that all five rhodococcal species produce structurally highly similar or identical hydroxamate compounds.

The bioinformatic and transcriptional analysis of the *rhbABCDE* cluster strongly suggested that it directs the synthesis of a siderophore. This was further supported by a mutational analysis of this cluster. Disruption of the *rhbCD* genes prevented growth of *R. equi* SID2 in the presence of low concentrations of the iron chelator 2,2-dipyridyl and, in addition, reduced the growth rate of this mutant in iron-depleted medium compared to that of the wild type. Addition of culture supernatant of the wild type grown in iron-depleted medium to that of *R. equi* SID2 restored

the growth rate of the latter to close to that of the wild type in a dose-dependent manner. These data, together with the bioinformatic analysis of the *rhbABCDE* cluster, lead us to conclude that these genes are required for the production of a diffusible hydroxamate siderophore, rhequichelin.

Transcription of the rhequichelin and related rhequibactin biosynthetic genes was strongly upregulated in the first 10 h following infection of nonactivated macrophages, suggesting that *R. equi* encounters iron restriction following macrophage infection. However, since *R. equi* proliferates in macrophages, it clearly is able to obtain sufficient iron for growth. We previously demonstrated that rhequibactin is not essential for virulence (30). However, disruption of the rhequichelin biosynthesis genes attenuated bacterial growth in macrophages, showing that iron acquisition in the phagosomal compartment in which *R. equi* resides is dependent on this siderophore. These observations correspond to those made for *Mycobacterium tuberculosis* and *Mycobacterium avium*. Infection of macrophages with these pathogens resulted in an increase in the phagosomal iron concentration, which was derived from transferrin. In sharp contrast, the iron concentration in phagosomes harboring the nonpathogenic *M. smegmatis* decreased following infection (49, 50). The ability of *M. tuberculosis* to proliferate in macrophages is dependent on the biosynthesis of the siderophore mycobactin (13); furthermore, the increase in phagosomal iron concentration seen following infection of macrophages with *M. tuberculosis* did not occur following infection with an *M. tuberculosis* strain unable to produce mycobactin (49). These data strongly suggest that mycobactin competes with transferrin for iron, preventing a decrease in the phagosomal iron concentration. The data presented here suggest that rhequichelin fulfills a role similar to that of mycobactin.

In addition to preventing proliferation in macrophages, disruption of rhequichelin biosynthesis also attenuated growth and survival of *R. equi* in SCID mice, resulting in clearance of the pathogen in lungs and a dramatic reduction in bacterial numbers in liver and spleen, further supporting the importance of this siderophore in virulence. In stark contrast, previous disruption of *iupS* or *iupU*, which are required for biosynthesis of rhequibactin and a nondiffusible siderophore, respectively, had no effect on the establishment of a chronic infection in mice (30). These data suggest that rhequichelin may have characteristics that make it better at obtaining iron from iron sources present in the phagosome than rhequibactin. The observation that a specific siderophore out of several is preferred in virulence has been described for a number of other pathogenic bacteria (8, 42, 47). Uropathogenic *E. coli* strains produce up to four siderophores: the catecholates enterobactin and salmochelin and the hydroxamates aerobactin and yersiniabactin. However, only the latter two contributed significantly to urinary tract infection, despite the fact that aerobactin has a lower affinity for iron than enterobactin (5, 17, 33, 34). In comparison to enterobactin, aerobactin preferentially derives iron from cell components, which may explain its role in virulence (5).

Comparative analysis of rhodococcal genomes showed that the pathogenic *R. equi* acquired only a few virulence-specific genes through horizontal gene transfer, most notably the pathogenicity island of the virulence plasmid. The majority of potential virulence-associated factors identified in the genome are also present in nonpathogenic *Rhodococcus* species, suggesting that *R. equi* virulence evolved by cooption of existing core actinobacterial traits which were not initially involved in virulence or which did not

evolve primarily to play a specific role in pathogenesis (24). The rhequichelin biosynthetic cluster is an excellent example of this: while a bioinformatic analysis provides strong evidence that nonpathogenic rhodococci produce rhequichelin or a structurally highly related compound, it clearly is indispensable for virulence of *R. equi* and hence is a virulence-associated factor.

REFERENCES

1. **Andrews SC, Robinson AK, Rodriguez-Quinones F.** 2003. Bacterial iron homeostasis. FEMS Microbiol. Rev. **27**:215–237.
2. **Barton MD, Hughes KL.** 1984. Ecology of *Rhodococcus equi*. Vet. Microbiol. **9**:65–76.
3. **Bell KS, Philp JC, Aw DWJ, Christofi N.** 1998. The genus *Rhodococcus*. J. Appl. Microbiol. **85**:195–210.
4. **Bosello M, Robbel L, Linne U, Xie X, Marahiel MA.** 2011. Biosynthesis of the siderophore rhodochelin requires the coordinated expression of three independent gene clusters in *Rhodococcus jostii* RHA1. J. Am. Chem. Soc. **133**:4587–4595.
5. **Brock JH, Williams PH, Liceaga J, Wooldridge KG.** 1991. Relative availability of transferrin-bound iron and cell-derived iron to aerobactin-producing and enterochelin-producing strains of *Escherichia coli* and to other microorganisms. Infect. Immun. **59**:3185–3190.
6. **Butcher PD, Mangan JA, Monahan IM.** 1998. Intracellular gene expression. Analysis of RNA from mycobacteria in macrophages using RT-PCR. Methods Mol. Biol. **101**:285–306.
7. **Carrano CJ, Jordan M, Drechsel H, Schmid DG, Winkelmann G.** 2001. Heterobactins: a new class of siderophores from *Rhodococcus erythropolis* IGTS8 containing both hydroxamate and catecholate donor groups. Biometals **14**:119–125.
8. **Cendrowski S, MacArthur W, Hanna P.** 2004. *Bacillus anthracis* requires siderophore biosynthesis for growth in macrophages and mouse virulence. Mol. Microbiol. **51**:407–417.
9. **Challis GL.** 2005. A widely distributed bacterial pathway for siderophore biosynthesis independent of nonribosomal peptide synthetases. Chembiochem **6**:601–611.
10. **Challis GL, Ravel J, Townsend CA.** 2000. Predictive, structure-based model of amino acid recognition by nonribosomal peptide synthetase adenylation domains. Chem. Biol. **7**:211–224.
11. **Conti E, Stachelhaus T, Marahiel MA, Brick P.** 1997. Structural basis for the activation of phenylalanine in the non-ribosomal biosynthesis of gramicidin S. EMBO J. **16**:4174–4183.
12. **Crosa JH, Walsh CT.** 2002. Genetics and assembly line enzymology of siderophore biosynthesis in bacteria. Microbiol. Mol. Biol. Rev. **66**:223–249.
13. **De Voss JJ, et al.** 2000. The salicylate-derived mycobactin siderophores of *Mycobacterium tuberculosis* are essential for growth in macrophages. Proc. Natl. Acad. Sci. U. S. A. **97**:1252–1257.
14. **Dhungana S, et al.** 2007. Purification and characterization of rhodobactin: a mixed ligand siderophore from *Rhodococcus rhodochrous* strain OFS. Biometals **20**:853–867.
15. **Felnagle EA, et al.** 2010. MbtH-like proteins as integral components of bacterial nonribosomal peptide synthetases. Biochemistry **49**:8815–8817.
16. **Fernandez-Mora E, Polidori M, Lührmann A, Schaible UE, Haas A.** 2005. Maturation of *Rhodococcus equi*-containing vacuoles is arrested after completion of the early endosome stage. Traffic **6**:635–653.
17. **Garcia EC, Brumbaugh AR, Mobley HL.** 2011. Redundancy and specificity of *Escherichia coli* iron acquisition systems during urinary tract infection. Infect. Immun. **79**:1225–1235.
18. **Giguère S, et al.** 1999. Role of the 85-kilobase plasmid and plasmid-encoded virulence-associated protein A in intracellular survival and virulence of *Rhodococcus equi*. Infect. Immun. **67**:3548–3557.

19. **Hondalus MK, Mosser DM.** 1994. Survival and replication of *Rhodococcus equi* in macrophages. Infect. Immun. **62:**4167–4175.

20. **Hughes KL, Sulaiman I.** 1987. The ecology of *Rhodococcus equi* and physicochemical influences on growth. Vet. Microbiol. **14:**241–250.

21. **Jain S, Bloom BR, Hondalus MK.** 2003. Deletion of *vapA* encoding virulence associated protein A attenuates the intracellular actinomycete *Rhodococcus equi*. Mol. Microbiol. **50:**115–128.

22. **Kelly BG, Wall DW, Boland CA, Meijer WG.** 2002. Isocitrate lyase of the facultative intracellular pathogen *Rhodococcus equi*. Microbiology **148:**793–798.

23. **Köster W.** 2001. ABC transporter-mediated uptake of iron, siderophores, heme and vitamin B12. Res. Microbiol. **152:**291–301.

24. **Letek M, et al.** 2010. The genome of a pathogenic rhodococcus: cooptive virulence underpinned by key gene acquisitions. PLoS Genet. **6:**e1001145. doi:10.1371/journal.pgen.1001145.

25. **Lin H, Fischbach MA, Liu DR, Walsh CT.** 2005. In vitro characterization of salmochelin and enterobactin trilactone hydrolases IroD, IroE, and Fes. J. Am. Chem. Soc. **127:**11075–11084.

26. **Lührmann A, et al.** 2004. Necrotic death of *Rhodococcus equi*-infected macrophages is regulated by virulence-associated plasmids. Infect. Immun. **72:**853–862.

27. **Mangan MW, Meijer WG.** 2001. Random insertion mutagenesis of the intracellular pathogen *Rhodococcus equi* using transposomes. FEMS Microbiol. Lett. **205:**243–246.

28. **Mies KA, Wirgau JI, Crumbliss AL.** 2006. Ternary complex formation facilitates a redox mechanism for iron release from a siderophore. Biometals **19:**115–126.

29. **Miranda-Casoluengo R, et al.** 2005. The iron-regulated *iupABC* operon is required for saprophytic growth of the intracellular pathogen *Rhodococcus equi* at low iron concentrations. J. Bacteriol. **187:**3438–3444.

30. **Miranda-Casoluengo R, Prescott JF, Vazquez-Boland JA, Meijer WG.** 2008. The intracellular pathogen *Rhodococcus equi* produces a catecholate siderophore required for saprophytic growth. J. Bacteriol. **190:**1631–1637.

31. **Muscatello G, et al.** 2007. *Rhodococcus equi* infection in foals: the science of 'rattles'. Equine Vet. J. **39:**470–478.

32. **Nagy I, et al.** 1995. Degradation of the thiocarbamate herbicide EPTC (S-ethyl dipropylcarbamothioate) and biosafening by *Rhodococcus* sp. strain NI86/21 involve an inducible cytochrome P-450 system and aldehyde dehydrogenase. J. Bacteriol. **177:**676–687.

33. **Neilands JB.** 1981. Microbial iron compounds. Annu. Rev. Biochem. **50:**715–731.

34. **Perry RD, Balbo PB, Jones HA, Fetherston JD, DeMoll E.** 1999. Yersiniabactin from *Yersinia pestis*: biochemical characterization of the siderophore and its role in iron transport and regulation. Microbiology **145:**1181–1190.

35. **Ratledge C.** 2007. Iron metabolism and infection. Food Nutr. Bull. **28:**S515–S523.

36. **Rausch C, Weber T, Kohlbacher O, Wohlleben W, Huson DH.** 2005. Specificity prediction of adenylation domains in nonribosomal peptide synthetases (NRPS) using transductive support vector machines (TSVMs). Nucleic Acids Res. **33:**5799–5808.

37. **Rohde KH, Abramovitch RB, Russell DG.** 2007. *Mycobacterium tuberculosis* invasion of macrophages: linking bacterial gene expression to environmental cues. Cell Host Microbe **2:**352–364.

38. **Röttig M, et al.** 2011. NRPSpredictor2—a web server for predicting NRPS adenylation domain specificity. Nucleic Acids Res. **39:**W362–W367.

39. **Russell DA, Byrne GA, O'Connell EP, Boland CA, Meijer WG.** 2004. The LysR-type transcriptional regulator VirR is required for expression of the virulence gene *vapA* of *Rhodococcus equi* ATCC 33701. J. Bacteriol. **186:**5576–5584.

40. **Sambrook J, Russell DW.** 2001. Molecular cloning: a laboratory manual, 3rd ed. Cold Spring Harbor Laboratory Press, Cold Spring Harbor, NY.

41. **Takai S, et al.** 1991. Association between a large plasmid and 15- to 17-kilodalton antigens in virulent *Rhodococcus equi*. Infect. Immun. **59:**4056–4060.

42. **Takase H, Nitanai H, Hoshino K, Otani T.** 2000. Impact of siderophore production on *Pseudomonas aeruginosa* infections in immunosuppressed mice. Infect. Immun. **68:**1834–1839.

43. **Toyooka K, Takai S, Kirikae T.** 2005. *Rhodococcus equi* can survive a phagolysosomal environment in macrophages by suppressing acidification of the phagolysosome. J. Med. Microbiol. **54:**1007–1015.

44. **van der Geize R, JWde Hessels GI, Grommen AW, Jacobs AA, Dijkhuizen L.** 2008. A novel method to generate unmarked gene deletions in the intracellular pathogen *Rhodococcus equi* using 5-fluorocytosine conditional lethality. Nucleic Acids Res. **36:**e151.

45. **van der Geize R, Dijkhuizen L.** 2004. Harnessing the catabolic diversity of rhodococci for environmental and biotechnological applications. Curr. Opin. Microbiol. **7:**255–261.

46. **Vishniac W, Santer M.** 1957. The thiobacilli. Microbiol. Rev. **21:**195–213.

47. **Visser MB, Majumdar S, Hani E, Sokol PA.** 2004. Importance of the ornibactin and pyochelin siderophore transport systems in *Burkholderia cenocepacia* lung infections. Infect. Immun. **72:**2850–2857.

48. **von Bargen K, Haas A.** 2009. Molecular and infection biology of the horse pathogen *Rhodococcus equi*. FEMS Microbiol. Rev. **33:**870–891.

49. **Wagner D, et al.** 2005. Elemental analysis of *Mycobacterium avium*-, *Mycobacterium tuberculosis*-, and *Mycobacterium smegmatis*-containing phagosomes indicates pathogen-induced microenvironments within the host cell's endosomal system. J. Immunol. **174:**1491–1500.

50. **Wagner D, et al.** 2006. Elemental analysis of the *Mycobacterium avium* phagosome in Balb/c mouse macrophages. Biochem. Biophys. Res. Commun. **344:**1346–1351.

51. **Wandersman C, Delepelaire P.** 2004. Bacterial iron sources: from siderophores to hemophores. Annu. Rev. Microbiol. **58:**611–647.

52. **Yu S, Fiss E, Jacobs WR, Jr.** 1998. Analysis of the exochelin locus in *Mycobacterium smegmatis*: biosynthesis genes have homology with genes of the peptide synthetase family. J. Bacteriol. **180:**4676–4685.

53. **Zhu W, et al.** 1998. Exochelin genes in *Mycobacterium smegmatis*: identification of an ABC transporter and two non-ribosomal peptide synthetase genes. Mol. Microbiol. **29:**629–639.